# Global shape processing involves feature-selective and feature-agnostic coding mechanisms

**Jason Bell** School of Psychology, University of Western Australia, Perth, WA, Australia
Research School of Psychology, Australian National University, Canberra, ACT, Australia

**Mimosa Forsyth** Research School of Psychology, Australian National University, Canberra, ACT, Australia

**David R. Badcock** School of Psychology, University of Western Australia, Perth, WA, Australia

**Frederick A. A. Kingdom** McGill Vision Research, Department of Ophthalmology, McGill University, Montreal, QC, Canada

**Recent research and modeling proposes that a closed shape is accurately described by both the curvature and angular location of its parts relative to the shape center, implying that the shape is coded along with its overall orientation. We tested this proposition. Radial frequency (RF) patterns were employed as stimuli as they can represent a range of familiar closed shapes and are processed globally. We measured a RF amplitude aftereffect (RFAAE) as a function of the shape orientation difference between adapt and test patterns of the same RF. For RF3 and RF4, RFAAEs were largest when adapt and test patterns were the same orientation, and then linearly decreased as the adaptor was rotated away from the test. RFAAEs did not, however, reach zero, instead plateauing significantly above zero. On the other hand, when adapt and test were of opposite luminance polarity, RFAAEs, although lower than same luminance-polarity RFAAEs, were invariant to differences between adapt and test orientations. Our findings provide evidence for two global shape mechanisms: one that is selective for shape orientation and luminance polarity, and one that is agnostic to these characteristics.**

## Introduction

As an individual moves through the environment, the shape of a stationary viewed object undergoes various transformations, including those due to changes in viewing distance, viewpoint, brightness, and orientation. Here we consider whether global shape encoding mechanisms are sensitive to changes in the overall orientation of a shape. Recent research (Anderson, Habak, Wilkinson, & Wilson, 2007; Bell, Dickinson, & Badcock, 2008; Habak, Wilkinson, Zakher, & Wilson, 2004) and modeling (Pasupathy & Connor, 2002; Poirier & Wilson, 2006) proposes that a closed shape is described by both the curvature (both sign and magnitude) and angular location of its parts relative to the shape's center, implying that the overall orientation of the shape is encoded along with the shape itself. This communication tests the proposition that closed shapes are coded selectively for their orientation.

Object recognition involves a series of stages, from the extraction of oriented edges and their integration into contours in V1 (Hubel & Wiesel, 1968; Kapadia, Westheimer, & Gilbert, 1999), to the encoding of contour curvatures in V2 and/or V4 (Muller, Wilke, & Leopold, 2009; Pasupathy & Connor, 1999, 2001), to the encoding of global shape information in V4 (Connor, 2004; Dumoulin & Hess, 2007; Gallant, Braun, & Van Essen, 1993; Wilkinson et al., 2000) and finally, to the holistic encoding of the object in lateral occipital cortex (LOC) (Kourtzi & Kanwisher, 2001; Lerner, Hendler, Ben-Bashat, Harel, & Malach, 2001; Murray & He, 2006). Moreover in humans it is known

Citation: Bell, J., Forsyth, M., Badcock, D. R., & Kingdom, F. A. A. (2014). Global shape processing involves feature-selective and feature-agnostic coding mechanisms. *Journal of Vision*, *14*(11):12, 1–14, http://www.journalofvision.org/content/14/11/12, doi:10.1167/14.11.12.

doi: 10.1167/14.11.12 Received April 14, 2014; published September 19, 2014 ISSN 1534-7362 

that detectors for the initial stages of shape coding, specifically lines (Clifford, Wenderoth, & Spehar, 2000; Westheimer & Beard, 1998) and curves (Bell, Gheorghiu, & Kingdom, 2009; Timney & Macdonald, 1978), and for the final stages, e.g., faces (Rhodes et al., 2004; Susilo, McKone, & Edwards, 2010), are selective for stimulus orientation. Thus while coding of stimulus orientation appears to be generic, the orientation selectivity of intermediate stages of shape processing has not been described. Recent masking (Bell & Badcock, 2008; Habak, Wilkinson, & Wilson, 2006; Habak et al., 2004) and adaptation studies (Anderson et al., 2007; Bell et al., 2008) have provided evidence that global shape detectors are at least broadly selective for shape orientation, although reports of significant aftereffects with random-orientation adapt and test shapes call this interpretation into question (Bell, Gheorghiu, Hess, & Kingdom, 2011; Bell, Wilkinson, Wilson, Loffler, & Badcock, 2009). We extend this previous work by precisely characterizing the orientation selectivity of global contour shape mechanisms. Our findings will be compared with previous published estimates for face, curvature and line orientation mechanisms.

Since the work of Attneave (1954) it is generally agreed that the shape of an object is a powerful cue for its recognition. But how is holistic shape information encoded? Based on the seminal work of Attneave (1954), Biederman (1987), Hoffman and Richards (1984), and subsequent research findings (Barenholtz, 2010; Bell, Badcock, Wilson, & Wilkinson, 2007; Bell, Hancock, Kingdom, & Peirce, 2010; Bertamini & Farrant, 2005; Kurki, Saarinen, & Hyvarinen, 2009; Loffler, Wilson, & Wilkinson, 2003; Poirier & Wilson, 2007), we know that the curved points of an outline shape are important encoding features, more so than the straight line features. In light of this work, two influential and biologically plausible models of shape representation have emerged. Pasupathy and Connor's model (2002) is based upon physiological recordings from curvature selective neurons in macaque V4 (Pasupathy & Connor, 1999, 2001). Connor and colleagues have subsequently extended this work to reveal the importance of acute curvatures (Carlson, Rasquinha, Zhang, & Connor, 2011). Poirier and Wilson (2006), on the other hand, developed a model to account for human psychophysical data involving radial frequency (RF) patterns, stimuli believed to elicit global processing. These models differ in origin but share a number of key assumptions. Firstly both models propose that shapes are efficiently and accurately represented by their curves, as evidenced by the studies cited above. Secondly, both models propose that the angular location of curved features relative to the object's center is a fundamental characteristic for representing shape. A polar-based representation has additional merits for constructing a size invariant mechanism. However, coding for the angular location of curved features requires shape-coding mechanisms to be shape-orientation selective. The current study tests that assumption and in doing so provides the first precise description of the orientation selectivity of a known globally processed shape.

A frequently used stimulus for investigating global shape processing is the RF pattern (Wilkinson, Wilson, & Habak, 1998). These patterns are constructed by sinusoidally modulating the radius of a smooth circle. By changing the frequency (integer numbers allow smooth contours) one can change the shape represented: e.g., RF3 (triangle), RF4 (square), RF5 (pentagon). Changing the phase of the modulation alters the orientation of the shape being represented: e.g., a triangle (RF3) can be depicted resting on its base or on its apex, depending on the phase of the modulator. Thus RF patterns afford precise control over the shape being represented (number of cycles), its salience (amplitude of modulation), and its shape orientation (phase). Evidence for global processing of RF patterns comes from a variety of paradigms, including near-threshold (Bell & Badcock, 2008; Dickinson, Han, Bell, & Badcock, 2010; Hess, Achtman, & Wang, 2001; Jeffrey, Wang, & Birch, 2002; Loffler et al., 2003) and supra-threshold (Bell, Wilkinson, et al., 2009; Schmidtmann, Kennedy, Orbach, & Loffler, 2012) sensitivity studies, masking (Bell, Wilkinson, et al., 2009; Habak et al., 2004), and subthreshold summation (Bell & Badcock, 2009) studies, and finally through studies of RF adaptation and associated aftereffects (Anderson et al., 2007; Bell et al., 2011; Bell & Kingdom, 2009).

The current study measured the size of a global shape aftereffect involving RF patterns, namely the radial frequency amplitude aftereffect, or RFAAE (Bell et al., 2011; Bell et al., 2010; Bell & Kingdom, 2009), as a function of the shape orientation difference between adapt and test patterns. Our results provide evidence for two global shape mechanisms: one that is selective for shape orientation and luminance polarity, as the literature predicts, and one that is agnostic to these characteristics. The significance of these findings is discussed in relation to current models of shape processing and the properties of higher (object) and lower (curvature and orientation) form processing mechanisms.

## General methods

### Participants

Four observers participated in this study; two were authors (JB and MF), while the other two (CH and FD) were naive as to the experimental aims of this study. All our main experiments included data from two naive observers; the control experiment in Figure 4 was the only exception to this, with one naive observer

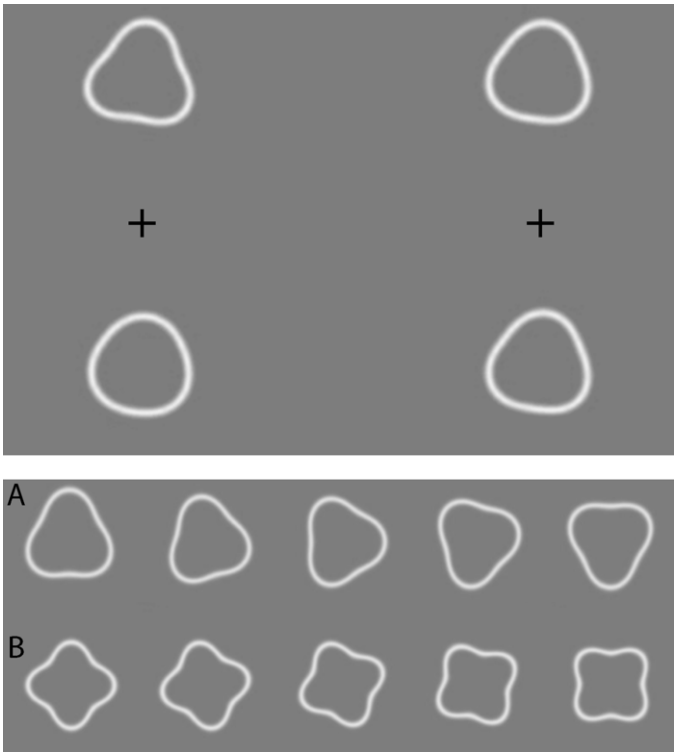


Figure 1. Top panel. A demonstration of the RFAAE. Observers attending to the fixation cross on the left will be adapted to a high amplitude (0.15) RF3 pattern in their upper visual field and a low amplitude (0.05) RF3 pattern in their lower visual field. Maintaining your gaze for 30 s is sufficient. To experience the RFAAE, move your gaze to the fixation cross on the right-hand side of Figure 1. Here the patterns in the upper and lower visual field have identical amplitudes but the observer may perceive the upper pattern to have lower amplitude, or appear more circular, than the lower pattern, which likely appears to have a higher amplitude, or be more deformed from circularity. This is the RFAAE. For simplicity, here the adapt and test patterns have the same radius, but in the experimental series the adapting patterns were 50% larger than the test patterns. Bottom panel. Row (A) shows the appearance of a high amplitude RF3 pattern as it is rotated in orientation through 60°. Row (B) shows the appearance of a high amplitude RF4 pattern as it is rotated in orientation through 45°.

only. All participants had normal or corrected-to-normal visual acuity. All participation was voluntary and unpaid. The protocol was approved by the Australian National University Human Ethics Committee and thus, accords with the conventions set out in the Declaration of Helsinki.

## Apparatus

Stimuli were created using the Matlab (version 7.11, Mathworks, Natick, MA) programming environment. Images were subsequently loaded through Cambridge Research system's Visage graphics system (Cambridge Research Systems, Ltd. [CRS], Rochester, UK) and displayed on a ViewSonic Professional Series PF817 monitor (ViewSonic Corporation, Walnut, CA). Screen resolution was 1024 × 768, with a refresh rate of 100 Hz and a mean luminance of 46.2 cd/m$^2$. The luminance display of the monitor was gamma corrected using a CRS optical device. The stimuli were presented at the viewing distance of 1.1 m, where each pixel subtended 1′ of visual angle, or 0.017°.

## Stimuli

Adaptation and test stimuli consisted of pairs of RF contours, example stimuli are shown in the top panel of Figure 1, and example adaptor orientations are shown in the bottom panel of the same figure. The RF contours were created by modulating the radius of a circle using the function set out by Wilkinson et al. (1998):

$$r(\theta) = r_{mean}\Big(1 + A\sin(\omega\theta + \varphi)\Big) \quad (1)$$

where $r$ (radius) and θ (angle) represent the polar coordinates of the contour and $r_{mean}$ is the average radius of the contour. $A$ is the amplitude of pattern deformation (between 0 and 1), $\omega$ is the RF number, and φ is the angular phase (orientation) of the shape.

## Procedure

A staircase procedure was used to measure the RFAAE (demonstrated in Figure 1). The procedure was the same as that used by Bell and Kingdom (2009).

In all conditions, individual adaptation and test stimuli were presented 3° above or below a central gray fixation cross. The spatial location of the patterns was independently spatially jittered ±0.5° on each trial to reduce the build-up of local orientation and position adaptation. The adaptation period lasted 60 s, during which the location of each pattern was individually spatially jittered every 0.5 s. The amplitudes of the adapting patterns were 0.05 and 0.15 ($A$ in Equation 1). The test cycle began with a blank screen for 400 ms, followed by a tone to signal the presentation of the test pair, which was displayed for 500 ms. A blank screen was then displayed for 100 ms, and finally a top-up adaptation for 2.5 s. There was at minimum, a 5–10 min break between runs; this was to allow the adaptation effects to dissipate, and to minimize carry-over effects to the next run.

Observers were instructed to select whether the upper or lower test pattern appeared higher in amplitude, or more deformed from circularity. Re-

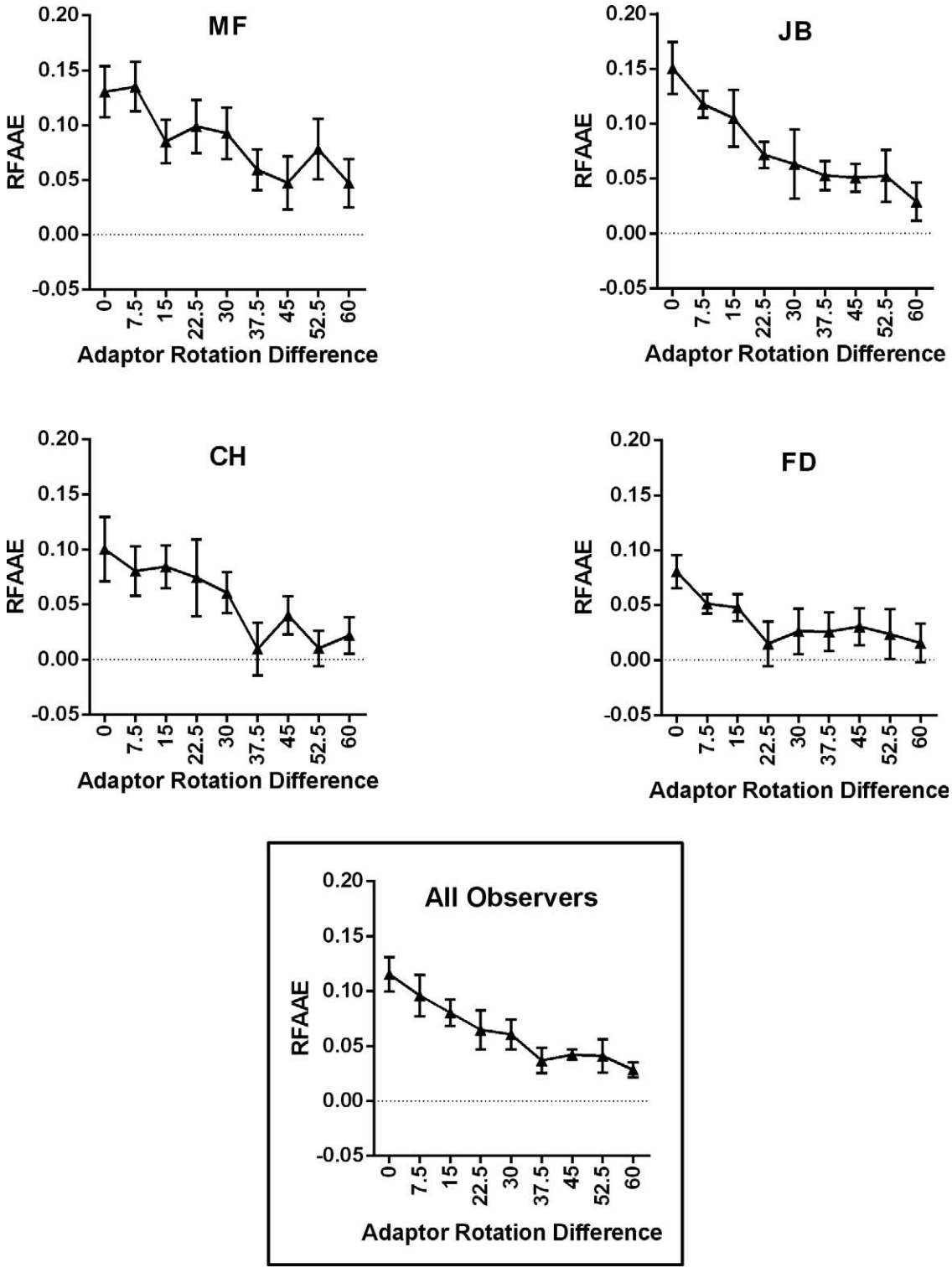


Figure 2. Panels 1–4 present RFAAEs for four observers as a function of the orientation difference between adaptor and test RF3s. The bottom boxed panel shows the averaged results for all observers. In each panel the vertical axis describes the size of the RFAAE and the horizontal axis describes the difference in the orientation of the adapting patterns relative to the fixed orientation test. Data points represent the $M \pm 1$ *SE*.

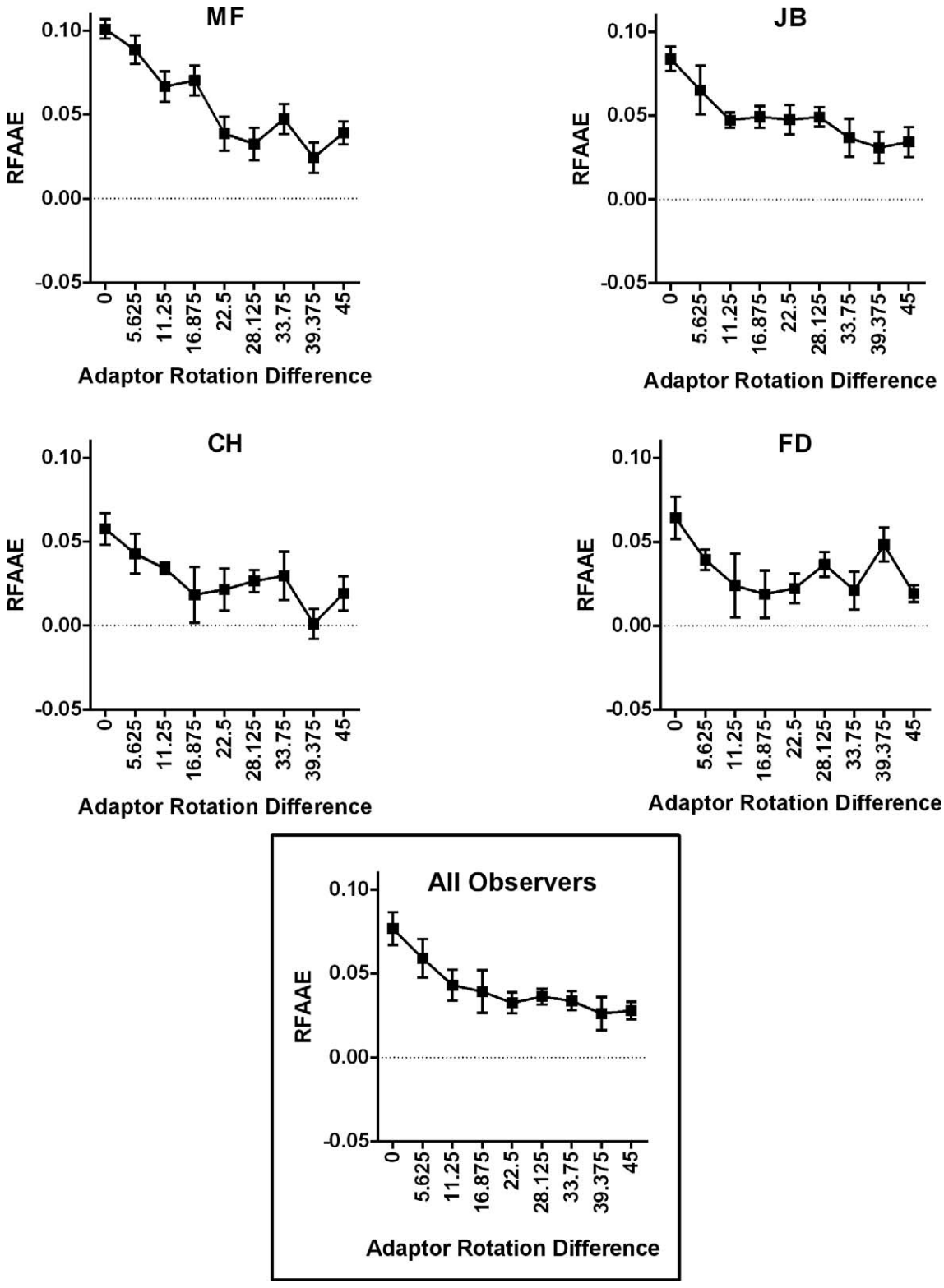


Figure 3. Panels 1–4 present RFAAEs for four observers as a function of the orientation difference between adaptor and test RF4s. The bottom boxed panel shows the averaged results for all observers. In each panel the vertical axis describes the size of the RFAAE and the horizontal axis describes the difference in the orientation of the adapting patterns relative to the fixed orientation test. Data points represent the $M \pm 1$ *SE*.

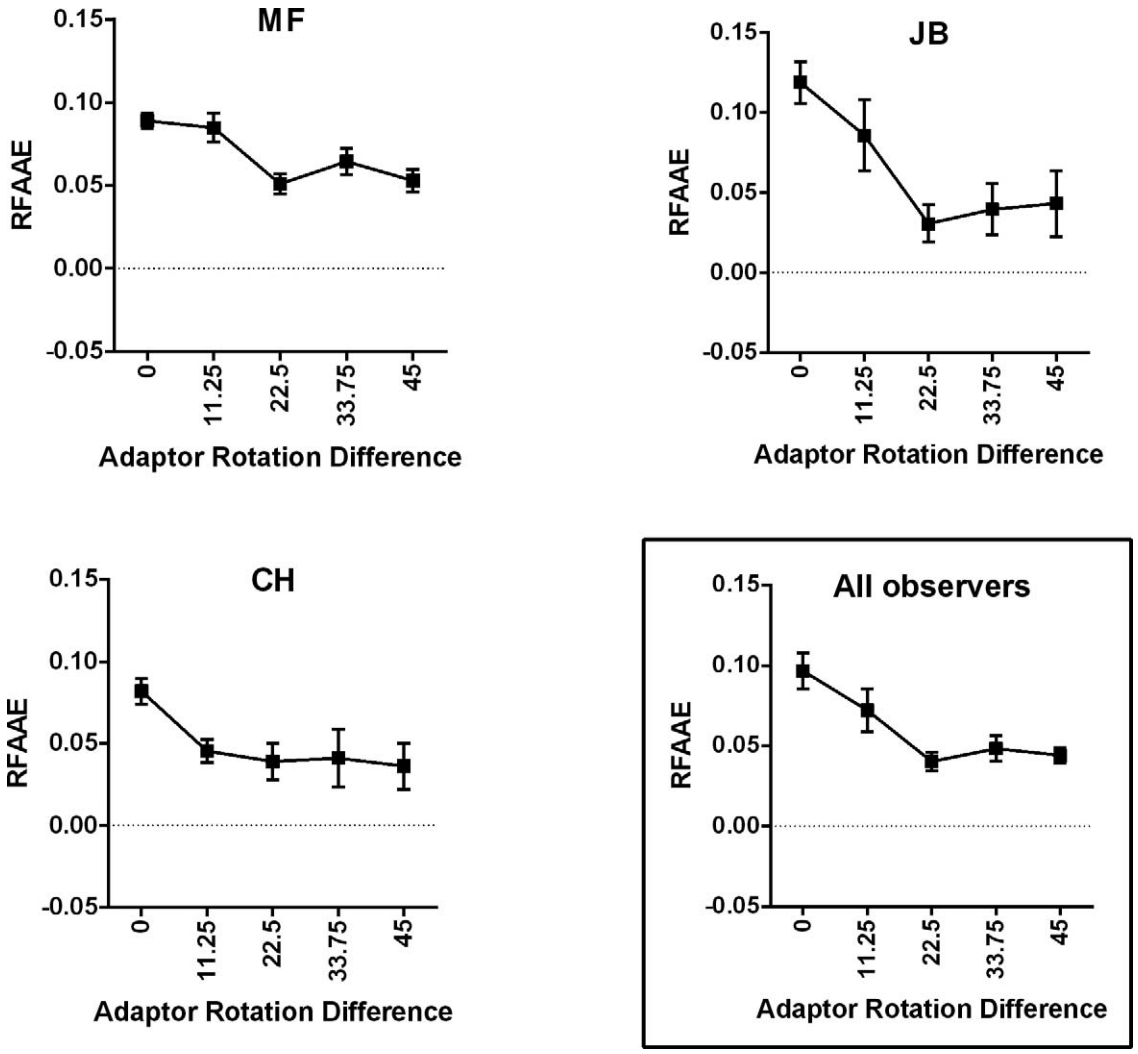


Figure 4. Control data with a differently oriented test. Panels 1–3 present RFAAEs for three observers as a function of the orientation difference between adaptor and test RF4s. The bottom right boxed panel shows the averaged results for all observers. In each panel the vertical axis describes the size of the RFAAE and the horizontal axis describes the difference in the orientation of the adapting patterns relative to the fixed orientation test. Data points represent the $M \pm 1$ *SE*.

sponses were made using a CB6 response box. This experiment was two-alternative-choice because although the observer was encouraged to make a choice, the next test pattern would appear whether the participant responded or not. This was to ensure that the duration of all runs was constant across experiments and participants, preventing the potentially confounding influence of decay of adaptation if some observers took longer to respond than others.

The amplitude ratio (upper divided by lower) of the test pair on the first trial was randomized between 0.8 and 1.2; this was to ensure that the observer could not predict the appropriate response on the first trial. Following each response the amplitude of the test patterns was adjusted in the direction opposite that of their response, i.e., towards the observer's point of subjective equality (PSE). For the first five trials the ratio of the test patterns was adjusted by a factor of 1.12, and then by a factor of 1.06 for the remaining 20 trials. The run ended after 25 trials and the PSE was calculated as the geometric mean of the ratio (upper amplitude divided by lower amplitude) of the test pattern amplitudes across the last 20 trials. Each run typically contained 6–10 response reversals.

Six PSEs were measured for each observer in each condition. In half the conditions the high-amplitude adapting pattern was in the upper visual field, and in the other half the low-amplitude adapting pattern was in the upper visual field. In addition the observers completed trials containing no adaptation stimulus; these runs were used as baselines with which to compare the size of the RFAAE with adaptation. The baseline trials were also used to control for biases in the upper or lower visual field. The size of the aftereffect in each condition was given by the ratio of the test amplitudes, at the PSE with adaptation, minus the PSE

without adaptation (baseline). For the figures the log of the ratios was used for each observer, meaning that zero represents no adaptation. The standard error of the mean across runs is given in each figure.

We took steps to ensure that the measured aftereffects were due to global shape rather than local orientation adaptation; in other words that they were not simply the sum of tilt aftereffects, or TAEs (Gibson & Radner, 1937), as has been suggested for some shape aftereffects (Blakemore & Over, 1974; Dickinson, Almeida, Bell, & Badcock, 2010; Dickinson, Mighall, Almeida, Bell, & Badcock, 2012). Studies have shown that if adapt and test stimuli differ in parameters such as position, luminance spatial-frequency, luminance polarity, temporal sequence, presentation eye, or size (radius), the involvement of TAEs is minimal (Anderson et al., 2007; Bell et al., 2008; Bell, Gheorghiu, et al., 2009; Bell & Kingdom, 2009; Burr & Ross, 2008; Gheorghiu & Kingdom, 2007b; Gheorghiu, Kingdom, Thai, & Sampasivam, 2009; Hancock & Peirce, 2008; Jeffery, Rhodes, & Busey, 2006; Rhodes et al., 2004; Timney & Macdonald, 1978). For both foveally viewed (Anderson et al., 2007) and peripherally viewed (Bell & Kingdom, 2009) stimuli—the latter analogous to those employed in the current study—a half degree difference in adapt and test radii appears to be sufficient to produce aftereffects of global shape not primarily mediated by local TAEs. Therefore by employing a radius change between adaptor and test as well as independent positional jitter for all patterns, we are confident that the aftereffects reported in this study are more likely to reflect adaptation of global shape than local orientation mechanisms.

# Experiments

## Experiment 1: Orientation selectivity of the global shape mechanism

Experiment 1 was designed to assess whether global shape mechanisms are selective for shape orientation, as predicted by recent models of shape processing (Pasupathy & Connor, 2002; Poirier & Wilson, 2006). We measured the size of a global shape aftereffect, the RFAAE (Bell & Kingdom, 2009), as a function of the difference in orientation between adaptor and test. We used RF3 (triangle-like shapes) and RF4 (square-like) shapes, both of which appear to evoke global processing (Bell & Badcock, 2009; Hess, Wang, & Dakin, 1999; Loffler et al., 2003). Test patterns were fixed in orientation and nine orientations of adaptor were employed in steps relative to the test and beginning at 0° of 7.5° for the RF3 and 5.625° for the RF4, culminating in orientation differences between adaptor and test of 60° and 45° respectively, the maximum obtainable. For the RF3 the maximally different orientation of 60° is a mirror-symmetric version of the original, i.e., an upside-down triangle adaptor with an upright triangle test. For the RF4 the maximally different orientation of 45° is a diamond-like adaptor with a square-like test. Given the special role of symmetrical counterparts shown in adaptation studies of shape parts (curves [Bell, Gheorghiu, et al., 2009] and inflections [Bell, Sampasivam, McGovern, Meso, & Kingdom, 2014]) we expected to find a difference between RF3 and RF4 in this final opposite condition, specifically greater aftereffects for the RF3.

### Results

Figures 2 and 3 show results for four observers for both RF3 and RF4. Each panel plots the size of the RFAAE as a function of the difference in orientation between adaptor and test. The bottom panel in each figure gives the average across all observers in each condition. Note the scale differences for RF3 and RF4 on both axes. For all observers, and for both pattern types, RFAAEs are largest when adaptor and test are the same orientation (0° difference) and decrease systematically as the adaptor is rotated away from the test. We conducted two tests. First we determined whether all the aftereffects were significantly different from zero (and thus informative) by performing a one-way repeated measures ANOVA including PSEs for baseline trials (no adaptation). The aftereffect was significant for both the RF3, $F(9, 27) = 17.64$, $p < 0.0001$, and RF4, $F(9, 27) = 7.29$, $p < 0.0001$. Bonferroni-corrected comparisons revealed that for RF3, all conditions except the 60° rotated condition were significantly different from baseline: i.e., eight of nine conditions showed significant adaptation. For RF4, the comparisons showed that all nine conditions were significantly different from baseline. Next, we carried out a repeated measures ANOVA on the adaptation conditions only to test whether the *decrease* in RFAAEs as a function of adapt-test orientation difference was significant: It is for both the RF3, $F(8, 24) = 14.58$, $p < 0.0001$, and RF4, $F(8, 24) = 7.801$, $p < 0.0001$. These results clearly demonstrate that global shape mechanisms are selective for shape orientation, as predicted.

Do the aftereffects uniformly decrease? To address this question we performed specific comparisons between adaptation conditions. We compared the aftereffects in each panel to the final condition, involving the largest orientation difference (60° for RF3; 45° for RF4). Aftereffects that differ significantly differ from these end points cannot be considered part of a plateau. For RF3, Bonferroni-corrected compar-

isons showed that the first four adaptation conditions involving small orientation differences (0°, 7.5°, 15°, and 22.5°) were significantly greater than the 60° condition while the remaining four, involving larger orientation differences, were not. This suggests that for RF3, the aftereffect plateaued in size when the orientation difference between adaptor and test was 30° or more. For RF4, Bonferroni-corrected comparisons showed that only two aftereffects (0° and 5.625°) were significantly greater than the 45° condition. This result suggests that for RF4, the plateau in aftereffect magnitude begins at a lesser 11.25°. Comparing the data for RF3 and RF4 may lead one to suggest that the shape-orientation bandwidths of distinct global RF shape mechanisms differ. We aim to explore this issue systematically across a range of RFs in future work.

Is there an alternative explanation for the data? It is possible that the decrease in RFAAE with adapt-test orientation difference happened because the adaptor became more obliquely oriented and as a result was coded less efficiently by the test mechanism, rather than because it was processed by a different mechanism to the test. To test this idea we reran the RF4 experiment using a test pattern that was oblique (45°), i.e., a diamond-like shape. The range of adaptor orientations was unchanged but we ran only every second condition, i.e., five conditions in total. Results for three observers are shown in Figure 4 and the average across observers is shown in the bottom right. To determine whether all the aftereffects were significantly different from zero (and thus informative) we performed a one-way repeated measures ANOVA with the baseline (no adaptation) PSEs as the other condition. This was significant, $F(5, 10) = 7.34$, $p < 0.01$, and Bonferroni-corrected comparisons confirmed that all five conditions were significantly different from baseline. Turning just to the adaptation conditions, the RFAAEs peak as before when adaptor and test are the same orientation and decline with orientation difference to around half the peak value and then plateau. This decrease was again significant, $F(4, 8) = 8.973$, $p < 0.005$, and Bonferroni-corrected comparisons showed that the 0° condition differed from the 45° condition, consistent with a peak followed by a plateau. The results thus mirror those obtained in the first two experiments and demonstrate that our result is not unique to a particular test shape orientation.

Finally we ran an analysis comparing the data in the two RF4 experiments (square- vs. diamond-like tests). This involved testing the matched conditions (i.e., using every second condition from the square-like test data in Figure 3) for the three observers who participated in both experiments. The analysis revealed a significant difference between the size of the aftereffects, $F(1, 2) = 28.73$, $p < 0.05$, but importantly, no interaction, $F(4, 8) = 0.72$, $p = 0.6$. This shows that RFAAEs were consistently larger when testing with a square-like RF4 test, than for a diamond-like RF4 test. More importantly though, rotating the adaptor away from the test had the same effect for both.

In both the above experiments the aftereffects do not decline to zero at large adaptor-test orientation differences; instead there appears to be a plateau beginning at around one third to one half of the maximum value. Thus there may be a mechanism that is adapted by a given shape (RF3 or RF4) but is *not* selective for the orientation relationship between adaptor and test. In the next experiment we explore whether such a shape mechanism is agnostic to other characteristics, such as luminance polarity.

## Experiment 2: Luminance-polarity specificity

Experiment 2 was designed to assess whether there exists a global-shape mechanism that is sensitive to luminance polarity. Previous work involving RF shapes has produced mixed reports, i.e., in favor (Bell et al., 2011; Hess et al., 2001) or against (Anderson et al., 2007; Bell & Badcock, 2008; Bell & Kingdom, 2009). The dependency of luminance-polarity sensitivity on shape orientation has not, however, been addressed, and in light of Experiment 1 could provide a resolution to these apparent discrepancies. Below we measure the size of the RFAAE for opposite polarity adapt and test patterns as a function of the orientation difference between the two.

## Results

The black square data points in Figure 5 shows averaged RFAAEs for four observers with a black adapting RF4 pattern and a white RF4 test, as a function of the orientation difference between the two. A one-way repeated measures ANOVA including baseline PSEs showed that there was a significant effect of adaptation, $F(5, 15) = 9.21$, $p < 0.0005$, and Bonferroni-corrected comparisons showed that all five adaptation conditions were significantly different from baseline. Next we compared the adaptation data. Although the data lacks the distinctive peak seen in the same polarity data (0° difference), there is nonetheless a small but significant effect of orientation on RFAAEs, $F(4, 12) = 3.57$, $p < 0.05$. However Bonferroni-corrected comparisons showed no significant differences between any adaptation condition and the final 45° condition. To put these results in context, Figure 5 also plots the same polarity data from Experiment 1 (gray square data points).

When adaptor and test are the same orientation, opposite luminance-polarity RFAAEs (black points)

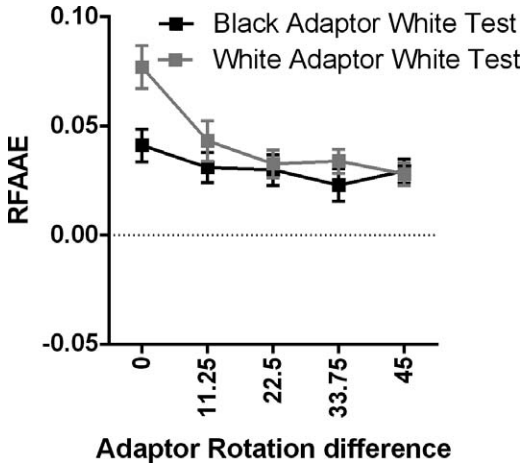


Figure 5. (A) Black square data points show opposite polarity RFAAEs averaged across four observers as a function of the orientation difference between adaptor and test. Data for the same observers under equivalent conditions with same polarity adapt and test patterns is shown in gray (replotted from Figure 3). In this Figure the vertical axis describes the size of the RFAAE and the horizontal axis describes the difference in the orientation of the adapting pattern relative to the fixed orientation test. Each data point represents the $M \pm 1$ *SE*.

are approximately half of those for same polarity (gray points), indicating selectivity for luminance polarity. However, the two data sets come together at around 11.25°. A two-way repeated measures ANOVA revealed an overall significant effect of polarity, $F(1, 3) = 15.06$, $p < 0.05$, and of orientation, $F(4, 12) = 35.3$, $p < 0.0001$, and not surprisingly a significant interaction between polarity and orientation, $F(4, 12) = 7.65$, $p < 0.01$. The interaction indicates that the effect of adaptor rotation on RFAAEs differed as a function of the polarity of the adaptor. Bonferroni-corrected comparisons demonstrated a large and significant difference between same- and opposite-polarity RFAAEs when adaptor and test were the same orientation. In contrast, there was no significant difference between same- and opposite-polarity RFAAEs for any of other orientation condition.

Taken together the results of Experiments 1 and 2 suggest that RF shape aftereffects are polarity selective when they are orientation selective and polarity insensitive when they are orientation insensitive. This dichotomy appears consistent with two distinct global shape-processing regimes.

## General discussion

The current study set out to test a prediction arising from recent studies (Anderson et al., 2007; Bell et al., 2008; Dickinson, Almeida, et al., 2010; Dickinson et al., 2012; Habak et al., 2006; Habak et al., 2004) and modeling work (Cadieu et al., 2007; Carlson et al., 2011; Pasupathy & Connor, 2002) concerning shape processing, namely that shape-coding mechanisms are selective for the location of the curved features of a shape, and therefore selective for the overall orientation of a shape. Consistent with this prediction, Experiment 1 found that RFAAEs were strongest when adaptor and test were of the same or similar orientation and then declined as the orientation difference increased. This is compelling evidence for shape–orientation-tuned mechanisms. Moreover, the same pattern of results was obtained for two distinct global shapes, RF3 (Figure 2) and RF4 (Figure 3), and for two different shape orientations, a square-like (0° rotated) and diamond-like (45° rotated) RF4 test (Figure 5). Taken together with previous findings showing that RF shape aftereffects, under appropriate circumstances, are RF shape specific (Anderson et al., 2007; Bell et al., 2008; Bell, Wilkinson, et al., 2009) and that different RFs can be discriminated perfectly at their thresholds for detection, meaning separate mechanisms must exist (Dickinson, Bell, & Badcock, 2013), we conclude that there exist mechanisms that code for a given global contour shape at a given shape orientation.

These findings accord with previous work showing that RF shape mechanisms are broadly orientation tuned (Bell & Badcock, 2008; Habak et al., 2004) but extend that work by more finely sampling the possible range of orientation misalignments. By doing so we have produced a detailed description of the orientation selectivity of the global shape mechanism that can be compared with other visual form mechanisms, as we do below. It is interesting to note, however, that while lateral masking studies reliably show no interaction between mask and test RF patterns that are 180° out-of-phase (Bell & Badcock, 2008; Habak et al., 2004), the data in this and other adaptation studies (Anderson et al., 2007) show strong global shape aftereffects for 180° out-of-phase adapt and test patterns. This issue warrants further investigation.

Orientation tuning has also been reported for shape parts, such as curves (Bell, Gheorghiu, et al., 2009; Timney & Macdonald, 1978). That is, it has been repeatedly shown that curvature-based aftereffects are strongly tuned for the curvature orientation relationship between adaptor and test. Moreover, for curves, no measurable aftereffect could be observed when adapt and test patterns differed in orientation by 45°; suggesting that the detectors for coding curves have narrow orientation tuning profiles (Bell, Gheorghiu, et al., 2009). Such findings accord with physiological reports for curvature orientation selective curvature detectors in macaque V4 (Pasupathy & Connor, 1999, 2001). In contrast, here we show that global shape aftereffects involving RF patterns remain significant

despite 45° orientation differences. This suggests important differences in the orientation tuning properties of detectors for curvature and global shape, respectively.

Before discussing the implications of a two-stage global-shape processing, it seems sensible to consider whether there are more simple explanations for our results. For instance can our results be explained by local curvature and/or orientation adaptation? As noted above, curvature aftereffects are abolished when adaptor and test differ in orientation by 45°. For the RF4 conditions, rotating the adaptor 45° relative to the test causes all local curves to differ in orientation by precisely 45°. Curvature aftereffects do not transfer across 45° and so the presence of significant RF shape aftereffects in such cases directly contradicts a local curvature adaptation explanation. Moreover, when the adaptor and test differ in size, as they do here, then their respective curvature features differ in width, also known as chord. Curvature based aftereffects are strongly selective for chord length (Gheorghiu & Kingdom, 2007a, 2007b) and transfer of any curvature aftereffects would be weak at best.

Can our findings be explained by local orientation adaptation? As discussed in detail in our procedure for Experiment 1, if the spatial correspondence between adaptor and test is reduced, then it is possible to measure aftereffects that are not primarily the result of local TAEs. We employed an appropriate radius change between adaptor and test patterns in addition to an independent spatial jitter of each pattern, for this purpose. And finally, it has been repeatedly shown that local TAEs for contour lines are insensitive to the luminance-polarity relationship between adapt and test lines (Bell et al., 2014; Magnussen & Kurtenbach, 1979). Clearly then, the luminance-polarity selective aftereffects reported here in cases where adapt and test are of same or similar orientation, cannot be explained by luminance-polarity insensitive local TAEs. These arguments relate to adaptation findings. Local polarity sensitivity can be seen in other paradigms (cf. Elder & Zucker, 1994; Spehar, 2002).

To that end, we observed luminance-polarity selective shape aftereffects when adapt and test shapes were the same orientation but no such selectivity when adapt and test orientations differed. Only one previous adaptation study (Bell & Kingdom, 2009) has directly examined the luminance-polarity selectivity of a global shape aftereffect under orientation-matched conditions, reporting weak or nonselectivity for the luminance-polarity relationship between adaptor and test under conditions of high spatial correspondence (small 0.25° spatial jitter or a size change). In the current study we report strong luminance-polarity selectivity for same orientation configurations, a seemingly contradictory result, but there is a key methodological difference. Here we have taken further steps to reduce spatial correspondence between adaptor and test by employing a larger spatial jitter and a size change rather than one or the other, as in previous work (Bell & Kingdom, 2009). Further demonstrating the importance of this correspondence for selectivity, even stronger selectivity for luminance polarity is observed for random phase configurations of the RFAAE (Bell et al., 2011; Bell & Kingdom, 2009). Thus, taken together these adaptation results may not be discrepant but instead, provide another demonstration of the importance of minimizing spatial correspondence between adapt and test patterns when measuring higher level visual aftereffects. Of course, this argument predicts that strong luminance-polarity selectivity should also be found when adapt and test patterns have fixed but different phases. That selectivity is not found under these circumstances is interesting because it suggests that a different process underpins adaptation transfer across differently oriented shapes.

This study presents evidence for a global shape mechanism that is agnostic to the orientation and luminance polarity of a shape. Ours is the first study to document insensitivity to both features in a single task, and extends previous work that has examined these questions in isolation. A recent study by Silson and colleagues (2013) showed that RF patterns activate the lateral occipital (LO) cortex, a high-level object selective region. These authors and others (Larsson & Heeger, 2006; Larsson, Landy, & Heeger, 2006), argue for an important subdivision of area LO: LO1 and LO2. Using transcranial magnetic stimulation (TMS), Silson and colleagues showed that TMS of LO2 impaired sensitivity to global RF shape but not orientation, while TMS to LO1 impaired sensitivity to orientation but not global shape: a clear double dissociation. The authors conclude that LO functionally subdivides into two: one area (LO2) selective for shape and the other (LO1) for orientation. Our findings accord with this view.

There is also previous work directly demonstrating a global RF shape mechanism that is insensitive to luminance polarity. Bell and Badcock (2008) have shown that RF patterns constructed from opposite-polarity contour segments have identical strengths of global integration to those constructed from same-polarity segments. Moreover the strength of masking observed between opposite- and same-polarity RF patterns is identical. The authors argue from these results that there are global RF shape mechanisms that are insensitive to the luminance polarity of the shape. Our adaptation results are consistent with that argument and extend the work to show that this global shape mechanism is also agnostic to the shape's

orientation. Thus the current study extends these singular examinations and by doing so, presents evidence for both feature-selective and feature-agnostic global shape mechanisms in human vision.

Reports of feature insensitivity extend beyond luminance polarity and shape orientation. The global RF shape mechanism has also been reported as insensitive to RF pattern size, luminance spatial-frequency profile, and to the order of the luminance statistics. Regarding size, adaptation studies have shown that RF shape aftereffects transfer strongly across adapt and test patterns that differ in size (Anderson et al., 2007; Bell et al., 2008; Bell, Wilkinson, et al., 2009) whilst remaining highly selective for adapt and test shape. Taken together with data showing RF sensitivity scales with pattern radius (Wilkinson et al., 1998), there is strong evidence for a size-invariant RF shape-coding mechanism. Regarding luminance spatial-frequency selectivity, adaptation studies have shown that under conditions of low spatial correspondence there is either a strong (Anderson et al., 2007) or complete (Bell & Kingdom, 2009) transfer of adaptation across conditions where adapt and test RFs differ in luminance spatial-frequency profile, relative to conditions where they do not, supporting a luminance spatial-frequency invariant coding mechanism. With regards to luminance statistics, it has been shown that the strength of global integration for RF shapes composed of luminance- and texture-defined parts is equal to that for shapes defined by luminance only (Bell & Badcock, 2008). Further, it was shown that a second-order texture-defined RF adaptor induces a significant aftereffect in a luminance-defined RF test that is equal to that for a luminance-defined adaptor (Bell, Wilkinson, et al., 2009). These sensitivity and adaptation findings argue for a global shape mechanism that is insensitive to the order of the luminance statistics. Adding our findings to these, we can conclude that there is evidence for a global shape coding mechanism that is selective for shape but is agnostic to that shape's: luminance polarity, luminance spatial-frequency profile, order of its luminance statistics (first- or second-order), size, and orientation.

While our data do not speak to the anatomical location of these distinct shape mechanisms, there are suggestions of anatomically distinct RF mechanisms from the imaging literature. Wilkinson et al. (2000) showed that RF patterns selectively activate area V4, an intermediate stage in the form processing pathway. Later work shows that RF patterns also activate a higher object selective region of the form pathway, namely area LO (Betts, Rainville, & Wilson, 2008; Silson et al., 2013). Given that LO2 appears to represent shape independent of orientation, it would be interesting to assess the luminance-polarity selectivity of the response in LO2 and see if it shows invariance. Finally, the current psychophysical model of RF shape perception (Poirier & Wilson, 2006) implicates area V4 but no higher-level mechanisms. Our findings imply the involvement of an additional mechanism and this is supported by recent fMRI work on RF patterns showing activation in area LO.

*Keywords: global, shape, orientation, adaptation, contour*

## Acknowledgments

This research was supported by an Australian Research Council (ARC) Discovery Project grant #DP110101511 given to JB, ARC grants DP1097003 and DP110104553 given to DRB, and a Natural Sciences and Engineering Research Council of Canada (NSERC) grant #RGPIN 121713-11 given to FK.

Commercial relationships: none.
Corresponding author: Jason Bell.
Email: jason.bell@uwa.edu.au.
Address: The University of Western Australia, School of Psychology, Crawley, Western Australia, Australia.

## References

Anderson, N. D., Habak, C., Wilkinson, F., & Wilson, H. R. (2007). Evaluating shape aftereffects with radial frequency patterns. *Vision Research*, *47*(3), 298–308.

Attneave, F. (1954). Some informational aspects of visual perception. *Psychological Review*, *61*(3), 183–193.

Barenholtz, E. (2010). Convexities move because they contain matter. *Journal of Vision*, *10*(11):19, 1–12, http://www.journalofvision.org/content/10/11/19, doi:10.1167/10.11.19. [PubMed] [Article]

Bell, J., & Badcock, D. R. (2008). Luminance and contrast cues are integrated in global shape detection with contours. *Vision Research*, *48*(21), 2336–2344.

Bell, J., & Badcock, D. R. (2009). Narrow-band radial frequency shape channels revealed by sub-threshold summation. *Vision Research*, *49*(8), 843–850.

Bell, J., Badcock, D. R., Wilson, H., & Wilkinson, F. (2007). Detection of shape in radial frequency contours: Independence of local and global form information. *Vision Research*, *47*(11), 1518–1522.

Bell, J., Dickinson, J. E., & Badcock, D. R. (2008). Radial frequency adaptation suggests polar-based coding of local shape cues. *Vision Research*, *48*(21), 2293–2301.

Bell, J., Gheorghiu, E., Hess, R. F., & Kingdom, F. A. A. (2011). Global shape processing involves a hierarchy of integration stages. *Vision Research*, *51*(15), 1760–1766.

Bell, J., Gheorghiu, E., & Kingdom, F. A. A. (2009). Orientation tuning of curvature adaptation reveals both curvature-polarity-selective and non-selective mechanisms. *Journal of Vision*, *9*(12):3, 1–11, http://www.journalofvision.org/content/9/12/3, doi:10.1167/9.12.3. [PubMed] [Article]

Bell, J., Hancock, S., Kingdom, F. A. A., & Peirce, J. W. (2010). Global shape processing: Which parts form the whole? *Journal of Vision*, *10*(6):16, 1–13, http://www.journalofvision.org/content/10/6/16, doi:10.1167/10.6.16. [PubMed] [Article]

Bell, J., & Kingdom, F. A. A. (2009). Global contour shapes are coded differently from their local components. *Vision Research*, *49*(13), 1702–1710.

Bell, J., Sampasivam, S., McGovern, D. P., Meso, A. I., & Kingdom, F. A. A. (2014). Contour inflections are adaptable features. *Journal of Vision*, *14*(7):2, 1–14, http://www.journalofvision.org/content/14/7/2, doi:10.1167/14.7.2. [PubMed] [Article]

Bell, J., Wilkinson, F., Wilson, H. R., Loffler, G., & Badcock, D. R. (2009). Radial frequency adaptation reveals interacting contour shape channels. *Vision Research*, *49*(18), 2306–2317.

Bertamini, M., & Farrant, T. (2005). Detection of change in shape and its relation to part structure. *Acta Psychologica (Amsterdam)*, *120*(1), 35–54.

Betts, L., Rainville, S., & Wilson, H. (2008). Adaptation to radial frequency patterns in the lateral occipital cortex. *Journal of Vision*, *8*(6):723, http://www.journalofvision.org/content/8/6/723, doi:10.1167/8.6.723. [Abstract]

Biederman, I. (1987). Recognition-by-components: A theory of human image understanding. *Psychological Review*, *94*(2), 115–147.

Blakemore, C., & Over, R. (1974). Curvature detectors in human vision? *Perception*, *3*(1), 3–7.

Burr, D., & Ross, J. (2008). A visual sense of number. *Current Biology*, *18*(6), 425–428.

Cadieu, C., Kouh, M., Pasupathy, A., Connor, C. E., Riesenhuber, M., & Poggio, T. (2007). A model of V4 shape selectivity and invariance. *Journal of Neurophysiology*, *98*(3), 1733–1750.

Carlson, E. T., Rasquinha, R. J., Zhang, K., & Connor, C. E. (2011). A sparse object coding scheme in area V4. *Current Biology*, *21*(4), 288–293.

Clifford, C. W., Wenderoth, P., & Spehar, B. (2000). A functional angle on some aftereffects in cortical vision. *Proceedings of the Royal Society B: Biological Sciences*, *267*(1454), 1705–1710.

Connor, C. E. (2004). Shape dimensions and object primitives. In L. M. Chalupa & J. S. Werner (Eds.), *The visual neurosciences* (pp. 1080–1089). London: MIT Press.

Dickinson, J. E., Almeida, R. A., Bell, J., & Badcock, D. R. (2010). Global shape aftereffects have a local substrate: A tilt aftereffect field. *Journal of Vision*, *10*(13):5, 1–12, http://www.journalofvision.org/content/10/13/5, doi:10.1167/10.13.5. [PubMed] [Article]

Dickinson, J. E., Bell, J., & Badcock, D. R. (2013). Near their thresholds for detection, shapes are discriminated by the angular separation of their corners. *PloS One*, *8*(5), e66015.

Dickinson, J. E., Han, L., Bell, J., & Badcock, D. R. (2010). Local motion effects on form in radial frequency patterns. *Journal of Vision*, *10*(3):20, 1–15, http://www.journalofvision.org/content/10/3/20, doi:10.1167/10.3.20. [PubMed] [Article]

Dickinson, J. E., Mighall, H. K., Almeida, R. A., Bell, J., & Badcock, D. R. (2012). Rapidly acquired shape and face aftereffects are retinotopic and local in origin. *Vision Research*, *65*, 1–11.

Dumoulin, S. O., & Hess, R. F. (2007). Cortical specialization for concentric shape processing. *Vision Research*, *47*(12), 1608–1613.

Elder, J., & Zucker, S. (1994). A measure of closure. *Vision Research*, *34*(24), 3361–3369.

Gallant, J. L., Braun, J., & Van Essen, D. C. (1993). Selectivity for polar, hyperbolic, and Cartesian gratings in macaque visual cortex. *Science*, *259*(5091), 100–103.

Gheorghiu, E., & Kingdom, F. A. (2007a). Chromatic tuning of contour-shape mechanisms revealed through the shape-frequency and shape-amplitude aftereffects. *Vision Research*, *47*(14), 1935–1949.

Gheorghiu, E., & Kingdom, F. A. (2007b). The spatial feature underlying the shape-frequency and shape-amplitude aftereffects. *Vision Research*, *47*(6), 834–844.

Gheorghiu, E., Kingdom, F. A., Thai, M. T., & Sampasivam, L. (2009). Binocular properties of curvature-encoding mechanisms revealed through two shape aftereffects. *Vision Research*, *49*(14), 1765–1774.

Gibson, J. J., & Radner, M. (1937). Adaptation, aftereffect and contrast in the perception of tilted lines. *Journal of Experimental Psychology*, *20*, 453–467.

Habak, C., Wilkinson, F., & Wilson, H. R. (2006). Dynamics of shape interaction in human vision. *Vision Research*, *46*(26), 4305–4320.

Habak, C., Wilkinson, F., Zakher, B., & Wilson, H. R. (2004). Curvature population coding for complex shapes in human vision. *Vision Research*, *44*(24), 2815–2823.

Hancock, S., & Peirce, J. W. (2008). Selective mechanisms for simple contours revealed by compound adaptation. *Journal of Vision*, *8*(7):11, 1–10, http://www.journalofvision.org/content/8/7/11, doi:10.1167/8.7.11. [PubMed] [Article]

Hess, R. F., Achtman, R. L., & Wang, Y. Z. (2001). Detection of contrast-defined shape. *Journal of the Optical Society of America A: Optics, Image Science, & Vision*, *18*(9), 2220–2227.

Hess, R. F., Wang, Y. Z., & Dakin, S. C. (1999). Are judgements of circularity local or global? *Vision Research*, *39*(26), 4354–4360.

Hoffman, D. D., & Richards, W. A. (1984). Parts of recognition. *Cognition*, *18*(1–3), 65–96.

Hubel, D. H., & Wiesel, T. N. (1968). Receptive fields and functional architecture of monkey striate cortex. *Journal of Physiology*, *195*(1), 215–243.

Jeffery, L., Rhodes, G., & Busey, T. (2006). View-specific coding of face shape. *Psychological Science*, *17*(6), 501–505.

Jeffrey, B. G., Wang, Y. Z., & Birch, E. E. (2002). Circular contour frequency in shape discrimination. *Vision Research*, *42*(25), 2773–2779.

Kapadia, M. K., Westheimer, G., & Gilbert, C. D. (1999). Dynamics of spatial summation in primary visual cortex of alert monkeys. *Proceedings of the National Academy of Sciences, USA*, *96*(21), 12073–12078.

Kourtzi, Z., & Kanwisher, N. (2001). Representation of perceived object shape by the human lateral occipital complex. *Science*, *293*(5534), 1506–1509.

Kurki, I., Saarinen, J., & Hyvarinen, A. (2009). Integration of contour features into a global shape: A classification image study. *Perception*, *38*, ECVP Abstract Supplement, 25.

Larsson, J., & Heeger, D. J. (2006). Two retinotopic visual areas in human lateral occipital cortex. *Journal of Neuroscience*, *26*(51), 13128–13142.

Larsson, J., Landy, M. S., & Heeger, D. J. (2006). Orientation-selective adaptation to first- and second-order patterns in human visual cortex. *Journal of Neurophysiology*, *95*(2), 862–881.

Lerner, Y., Hendler, T., Ben-Bashat, D., Harel, M., & Malach, R. (2001). A hierarchical axis of object processing stages in the human visual cortex. *Cerebral Cortex*, *11*(4), 287–297.

Loffler, G., Wilson, H. R., & Wilkinson, F. (2003). Local and global contributions to shape discrimination. *Vision Research*, *43*(5), 519–530.

Magnussen, S., & Kurtenbach, W. (1979). A test for contrast-polarity selectivity in the tilt aftereffect. *Perception*, *8*(5), 523–528.

Muller, K. M., Wilke, M., & Leopold, D. A. (2009). Visual adaptation to convexity in macaque area V4. *Neuroscience*, *161*(2), 655–662.

Murray, S. O., & He, S. (2006). Contrast invariance in the human lateral occipital complex depends on attention. *Current Biology*, *16*(6), 606–611.

Pasupathy, A., & Connor, C. E. (1999). Responses to contour features in macaque area V4. *Journal of Neurophysiology*, *82*(5), 2490–2502.

Pasupathy, A., & Connor, C. E. (2001). Shape representation in area V4: Position-specific tuning for boundary conformation. *Journal of Neurophysiology*, *86*(5), 2505–2519.

Pasupathy, A., & Connor, C. E. (2002). Population coding of shape in area V4. *Nature Neuroscience*, *5*(12), 1332–1338.

Poirier, F. J. A. M., & Wilson, H. R. (2006). A biologically plausible model of human radial frequency perception. *Vision Research*, *46*(15), 2443–2455.

Poirier, F. J. A. M., & Wilson, H. R. (2007). Object perception and masking: Contributions of sides and convexities. *Vision Research*, *47*(23), 3001–3011.

Rhodes, G., Jeffery, L., Watson, T. L., Jaquet, E., Winkler, C., & Clifford, C. W. (2004). Orientation-contingent face aftereffects and implications for face-coding mechanisms. *Current Biology*, *14*(23), 2119–2123.

Schmidtmann, G., Kennedy, G. J., Orbach, H. S., & Loffler, G. (2012). Non-linear global pooling in the discrimination of circular and non-circular shapes. *Vision Research*, *62*, 44–56.

Silson, E. H., McKeefry, D. J., Rodgers, J., Gouws, A. D., Hymers, M., & Morland, A. B. (2013). Specialized and independent processing of orientation and shape in visual field maps LO1 and LO2. *Nature Neuroscience*, *16*(3), 267–269.

Spehar, B. (2002). The role of contrast polarity in perceptual closure. *Vision Research*, *42*(3), 343–350.

Susilo, T., McKone, E., & Edwards, M. (2010). Solving the upside-down puzzle: Why do upright and inverted face aftereffects look alike? *Journal of Vision*, *10*(13):1, 1–16, http://www.journalofvision.org/content/10/13/1, doi:10.1167/10.13.1. [PubMed] [Article]

Timney, B. N., & Macdonald, C. (1978). Are curves detected by 'curvature detectors'? *Perception*, *7*(1), 51–64.

Westheimer, G., & Beard, B. L. (1998). Orientation dependency for foveal line stimuli: Detection and intensity discrimination, resolution, orientation discrimination and vernier acuity. *Vision Research*, *38*(8), 1097–1103.

Wilkinson, F., James, T. W., Wilson, H. R., Gati, J. S., Menon, R. S., & Goodale, M. A. (2000). An fMRI study of the selective activation of human extrastriate form vision areas by radial and concentric gratings. *Current Biology*, *10*(22), 1455–1458.

Wilkinson, F., Wilson, H. R., & Habak, C. (1998). Detection and recognition of radial frequency patterns. *Vision Research*, *38*(22), 3555–3568.